ISSN 1807-1929
Revista Brasileira de Engenharia Agrícola e Ambiental
Brazilian Journal of Agricultural and Environmental Engineering
v.30, n.9, e302061, 2026
Campina Grande, PB – http://www.agriambi.com.br – http://www.scielo.br/rbeaa

DOI: https://doi.org/10.1590/1807-1929/agriambi.v30n9e302061 ORIGINAL ARTICLE

Hysteresis in on-off pH control in *Scenedesmus obliquus* BR003 microalgae cultivation[1]

Histerese no controle liga-desliga de pH no cultivo da microalga *Scenedesmus obliquus* BR003

Euler M. de Souza[2], João V. P. Oliveira[2*], Pedro H. do Carmo[2], Dilson N. Rocha[2] & Marcio A. Martins[2]

[1] Research developed at Universidade Federal de Viçosa - UFV, Viçosa, Minas Gerais, Brazil
[2] Universidade Federal de Viçosa - UFV, Viçosa, Minas Gerais, Brazil

HIGHLIGHTS:

A narrow pH window (7.0–8.0) with moderate hysteresis of 0.5 improves Scenedesmus obliquus *microalgae growth.*
Growth was significantly reduced when pH values of the culture exceeded 8.0 or dropped below 6.5.
A growth medium 7.5 pH setpoint with 0.5 hysteresis reduces energy use in on-off control systems.

ABSTRACT: Microalgae cultivation efficiency depends on precise pH control via carbon dioxide injection. Optimizing these automated systems maximizes biomass and minimizes energy costs while enhancing sustainable carbon sequestration. This study evaluated the effect of hysteresis in pH control on *Scenedesmus obliquus* cultures using 6 L benchtop photobioreactors over 36 days. The cultures were maintained with commercial fertilizers under a light intensity of 134.82 μmol m^{-2} s^{-1} and a maximum CO_2 flow rate of 2 L h^{-1}. Growth kinetics were monitored via optical density at 680 nm (photosynthetic activity) and 750 nm (biomass accumulation), and data were modeled using a non-linear logistic regression. A binary control logic was explored to identify the optimal hysteresis and pH range. Duplicate cultures were evaluated in two procedures. Procedure one investigated three pH ranges (pH 7.0–8.0, 6.5–8.5, and 6.0–9.0) with hysteresis values of 0.5, 1.0, and 1.5. Procedure two evaluated dry mass production by maintaining a 0.5 hysteresis while shifting the reference value within the 6.5–8.5 range. Results indicated that extreme pH values (> 8.0 or < 6.5) significantly impaired growth, directly affecting carbon assimilation and inducing biological stress. A clear trade-off was identified: while the 6.5–7.5 range with 0.5 hysteresis provided the highest cell growth (maximum dry biomass of 1.02 g L^{-1}), the 7.0–8.0 range (7.5 setpoint) with 0.5 hysteresis was significantly superior regarding energy consumption efficiency.

Key words: photobioreactor, operational range, carbon dioxide injection, dry biomass, photosynthetic efficiency

RESUMO: A eficiência do cultivo de microalgas depende do controle preciso do pH por injeção de CO_2. A otimização desses sistemas maximiza a biomassa, minimiza custos energéticos e potencializa o sequestro sustentável de carbono. Este estudo avaliou o efeito da histerese no controle de pH em culturas de *Scenedesmus obliquus* em fotobiorreatores de bancada de 6 L ao longo de 36 dias. Os cultivos foram mantidos com fertilizantes comerciais sob intensidade luminosa de 134,82 μmol m^{-2} s^{-1} e vazão máxima de CO_2 de 2 L h^{-1}. A cinética de crescimento foi monitorada por densidade óptica a 680 nm (atividade fotossintética) e 750 nm (acúmulo de biomassa), modelada por regressão logística não linear. Uma lógica de controle binária foi explorada para identificar a histerese e a faixa de pH ideais. Culturas em duplicata foram avaliadas em dois procedimentos: o primeiro investigou três faixas de pH (7,0–8,0; 6,5–8,5 e 6,0–9,0) com histereses de 0,5, 1,0 e 1,5; o segundo avaliou a produção de massa seca mantendo histerese de 0,5 e variando o valor de referência na faixa 6,5–8,5. Os resultados indicaram que valores extremos de pH (> 8,0 ou < 6,5) prejudicaram significativamente o crescimento, afetando a assimilação de carbono e induzindo estresse biológico. A faixa 6,5–7,5 com histerese de 0,5 proporcionou o maior crescimento celular (biomassa seca máxima de 1,02 g L^{-1}), enquanto a faixa 7,0–8,0 (valor de referência de 7,5) com histerese de 0,5 foi superior em eficiência de consumo energético.

Palavras-chave: fotobiorreator, faixa operacional, injeção de dióxido de carbono, biomassa seca, eficiência fotossintética

Ref. 302061 – Received 20/10/2025
* Corresponding author - E-mail: oliveira.jvp@ufv.br
• Accepted 26/05/2026 • Published 27/08/2026
Editors: Antônio Gustavo de Luna Souto & Walter Esfrain Pereira

Publisher's Note: The statements, opinions, and data contained in this article are the sole responsibility of the author(s). The Agriambi Journal and/or Editor(s) disclaim any liability for damages to persons or property resulting from any ideas, methods, instructions, or products mentioned in the article.

This is an open-access article distributed under the Creative Commons Attribution 4.0 International License.

Introduction

Reducing emissions and enhancing carbon retention are central challenges in addressing climate change (Sierra et al., 2021). Despite a diversifying global energy mix, heavy reliance on fossil fuels remains a major source of CO_2 emissions (Tarafdar et al., 2023; Udaypal et al., 2024). Consequently, microalgae have emerged as a promising alternative for carbon sequestration. Capturing CO_2 more efficiently than trees, they offer potential applications in food, pharmaceuticals, and biofuels without competing for agricultural land, easily integrating into emission mitigation and wastewater treatment (Prasad et al., 2021; Ildefonso et al., 2026; Wang et al., 2025).

Among various species, *Scenedesmus obliquus* is widely studied due to its high growth rate, environmental robustness, and strong potential for CO_2 fixation and biomass production (Ildefonso et al., 2026). These traits make it an ideal model organism for evaluating process control variables like pH. Understanding its physiological mechanisms for CO_2 assimilation is essential for optimizing cultivation, as confirmed by Kong et al. (2021) and Prasad et al. (2021). Advances in cultivation integration continually improve the feasibility of large-scale applications (Huang et al., 2017; Borowiak et al., 2020).

Cultivation productivity is heavily influenced by pH, frequently reported as the most critical parameter (Tripathi et al., 2015; Isiramen et al., 2022; Khan et al., 2024). Optimal pH directly impacts cell growth and photosynthetic efficiency (Maghzian et al., 2024). Furthermore, pH is intrinsically linked to carbon supply: since current atmospheric CO_2 concentrations (~0.042%) are insufficient for dense cultures, supplementary CO_2 (~1-5%) must be injected (Qin et al., 2023; Wang et al., 2023; Lan et al., 2026). Rapid acidification upon CO_2 dissolution makes pH the primary variable for gas dosing control.

While most research focuses on static pH setpoints, this study innovates by exploring dynamic control mechanisms, such as hysteresis, to prevent gas waste, reduce costs, and mitigate biological stress. Although on-off systems with hysteresis are popular in automated systems to reduce actuator wear (Ogata, 2011; Simonová et al., 2017; Caparroz et al., 2024), their specific biological effects on pH regulation and microalgal growth remain underexplored (Molina et al., 2001; Mubarak et al., 2019).

This study hypothesizes that an optimally configured hysteresis band in on-off control enhances carbon uptake and overall biomass yield. Therefore, this study aims to investigate the influence of hysteresis band width in on-off pH control systems on the stability and yield of *Scenedesmus obliquus* cultures, contributing to improved process automation and operational efficiency.

Material and Methods

The research was conducted from May 1 to August 31, 2025, at the Biofuels Laboratory, part of the Department of Agricultural Engineering (DEA) at the Federal University of Viçosa (UFV), located in Viçosa, Minas Gerais, Brazil 20° 45' 14" S, 42° 52' 54" W), altitude of 648 m above sea level.

The microalgae used in this study, *Scenedesmus obliquus* BR003, were obtained from a laboratory culture collection. The culture media were sterilized in an autoclave at 1 atm and 121 °C for 20 min, following the protocol by Andersen (2005). Six bench-scale photobioreactors were used, each with a working volume of 6 L (5 L of culture medium and 1.0 L of inoculum). The photobioreactors were placed on a bench, and the entire system was kept isolated using cotton plugs to prevent contamination while allowing for gas exchange for aeration and carbon dioxide injection. The culture medium was prepared using tap water to better represent large-scale cultivation conditions. The medium was supplemented with commercial agricultural fertilizers, based on the formulation by Rocha et al. (2019), with the following concentrations (mg L^{-1}): urea (46% N) – 171.1; monoammonium phosphate (11% N and 22% P) – 44.4; potassium chloride (50% K) – 176.3; magnesium sulfate heptahydrate (9.8% Mg) – 46.0; and iron sulfate monohydrate (30% Fe) – 14.6.

The pH sensor used was the rechargeable model K38-1460 (KASVI, São José dos Pinhais, Brazil). The sensor was calibrated using certified buffer solutions (Êxodo Científica, Sumaré, Brazil) with pH values of 4.01 ± 0.02, 6.86 ± 0.02 and 10.04 ± 0.02. Although three buffers were used, the mathematical model was based on a two-point linear regression using the 4.01 and 6.86 standards. This approach was chosen because it minimized residual errors within the experimental range (pH 6.5 to 8.5). A quantitative error analysis revealed that forcing a 3-point linear regression (incorporating the pH 10.04 standard) introduced a substantial residual error of approximately 0.18 pH units exactly at the 6.86 calibration point, due to the sensor's inherent non-linearity within the highly alkaline range. By utilizing the 2-point model, this error at the neutral point was reduced to near zero, providing higher stability near the neutral point and displacing potential non-linearity errors to the unused upper range (pH 10).

The data from the calibration were used to calculate the slope, intercept, and pH, as described in Eqs. 1, 2, and 3. In this context, Oi denotes the electrical voltage offset corresponding to sensor i (where: i = 1, 2, …, 6), while the scaling factor of 3 accounts for the signal conditioning circuit's hardware gain.

$$\text{Slope} = \frac{(7.0 - 4.0) \times 3}{(\text{pH7 voltage} - \text{Oi}) - (\text{pH4 voltage} - \text{Oi})} \quad (1)$$

$$\text{Intercept} = 7.0 - \text{slope} \times \frac{\text{pH7 voltage} - \text{Oi}}{3} \quad (2)$$

$$\text{pH} = \frac{(\text{pH voltage} - \text{Oi})}{3} + \text{intercept} \quad (3)$$

Where:
Slope - pH sensor slope;
Intercept - pH sensor intercept; and,
Oi - voltage offset of each pH sensor.

After obtaining the slope, intercept, and pH, the sensor was validated using certified buffer solutions with known

pH values (pH 4.01, 6.86, and 10.04). The validation and subsequent adjustment procedures were carried out in accordance with the manufacturer's guidelines (KASVI, São José dos Pinhais, Brazil) and established electrochemical methodologies for pH electrode calibration and one-point offset correction (Galster, 1991; Skoog et al., 2013). The results were then used to adjust the sensor's offset. The offset is a constant value added to the sensor's output to compensate for the difference between the true and measured pH. This adjustment is crucial for accurate and reliable pH measurement, as the relationship between hydrogen and hydroxyl ion concentrations is complex. The offset is typically calculated based on the sensor's characteristics and is fine-tuned during calibration to ensure precise reading.

According to international standards EN ISO 10523 (ISO, 2008) and DIN 19266 (DIN, 2015), the pH of standard buffer solutions is defined at a reference temperature of 25 °C. For example, a pH 7.000 buffer solution at 25 °C has a pH of 7.016 at 20 °C, while a pH 4.005 buffer solution at 25 °C has a pH of 4.001 at 20 °C.

The pH probe was calibrated with two buffer solutions at 25 °C, yielding the linear relationship pH (pH_{25} = Slope × (Voltage−Sensor Offset) + InterceptpH_{25}. Since electrode slope is temperature-dependent according to the Nernst equation, readings for solutions between 20 and 25 °C were corrected using the temperature measured by a DS18B20 sensor. Considering the narrow temperature range, a linear approximation of the slope variation was adopted. A correction factor (CF) was calculated based on the slope difference between 25 and 20 °C (Eq. 4) and applied linearly to the measured temperature (Eq. 5). The corrected pH was then obtained by adding this factor to the calibrated reading (Eq. 6) (Galster, 1991; Skoog et al., 2013). This process automatically adjusts the pH reading to the actual solution temperature, ensuring accurate measurements within the 20–25 °C range.

$$CF_{max} = pH_{25}\left(\frac{S_{25}}{S_{20}} - 1\right) \approx 7 \times \left(\frac{59.16}{58.0} - 1\right) \approx 0.14 \quad (4)$$

$$CF(T) = \frac{25 - T}{5} \times CF_{max} \quad (5)$$

$$pH_{corrected} = pH_{25} + CF(T) \quad (6)$$

Where:

CF - temperature correction factor for the pH measurement;

CF_{max} - maximum correction factor calculated from the slope ratio of the pH sensor between 20 and 25 °C, and,

$pH_{corrected}$ - pH value corrected for temperature using the measured temperature T.

A total of six pH meters were calibrated as described by Khan et al. (2024). PH-4502C modules were used to condition the analog signal from the pH probes. These modules output positive voltages for pH values below 7 and negative voltages for pH values above 7. To enable reading by the Arduino microcontroller's (Mega 2560, Ivrea, Italy) analog inputs, which do not support negative voltages, the modules' integrated offset potentiometers were adjusted. This adjustment shifted the output to the positive range, with offset values set to approximately 2.5 V. Experimental pairs of voltage vs. pH were then recorded for each sensor, resulting in a calibration curve in the form of Eq. 7.

$$Y = -\text{slope}\ X + \text{intecept} \quad (7)$$

Where:

Y - pH value, and,

X - sensor's output voltage.

The negative slope of the calibration equation indicates that the sensor's output voltage decreases as pH increases. This inverse relationship between hydrogen ion concentration and generated potential is consistent with the typical electrochemical response of sensors based on glass and silver/silver chloride (Ag/AgCl) reference electrodes (Galster, 1991; Skoog et al., 2013).

During data acquisition, oscillations (noise) were observed in the pH values. This is a common phenomenon in electrochemical sensors, caused by environmental interference and electronic system limitations. To mitigate these variations and ensure greater reading stability, a digital moving average filter was implemented, similar to the one applied by Purnamasari et al. (2021), to reduce electronic noise and stabilize digital signals from other high-oscillation sensors (echo and temperature), demonstrating its reliability for data conditioning in microcontrollers. The filter used for the present work takes a total of 101 samples, with a 10-millisecond interval between readings.

Figure 1 shows the schematic of the experimental system. Six flasks were used, numbered S1 to S6, with three serving as primary cultures and the others as experimental duplicates.

The light source consisted of four 18W LED lamps, each with a luminous flux of 1850 lumens. Positioned at an average distance of 20 cm from the photobioreactors, this setup provided a photosynthetically active radiation (PAR) of 134.82 μmol m^{-2} s^{-1}. Although light saturation for *Scenedesmus obliquus* has been reported at 200–500 μmol m^{-2} s^{-1} under optimized conditions (Griffiths et al., 2011; Maghzian et al., 2024), moderate irradiance (100–150 μmol m^{-2} s^{-1}) is typically employed in laboratory-scale systems, where light attenuation and self-shading reduce the effective irradiance within the culture, allowing stable growth while minimizing photoinhibition. This range is consistent with conditions adopted in previous laboratory studies with *Scenedesmus*, including those conducted by our research group (Rocha et al., 2019; Rocha et al., 2023). Aeration was supplied by compressors. Inside each flask, the following components were installed: a pH sensor; a hose for CO_2 injection, connected to a porous stone to create microbubbles; and a hose connected to an air compressor for oxygenation. The flasks at the ends of the setup were also equipped with temperature sensors (two sensors for duplicate measurement, separated to verify temperature uniformity along the flask line).

Carbon dioxide (CO_2) was injected into the culture medium from a pressurized cylinder maintained at 1 Bar.

The gas flow was regulated by a needle valve. Due to pressure fluctuations in the shared distribution line caused by the automated valve actuations, a constant flow could not be maintained; however, the needle valve ensured a maximum flow rate of 2 L h^{-1}. CO_2 injection was controlled by a solenoid valve, which was automatically activated based on the pH measurement. The system operated under an on-off control logic with hysteresis.

To study hysteresis, control limits for the pH variable were established as an upper and a lower limit. The difference between these two limits relative to the setpoint determined the hysteresis value used in the system. The setpoint was fixed at pH 7.5, which corresponds to the cytosolic pH of microalgae, as described by Tripathi et al. (2015).

Based on this configuration, the controller operated in a binary fashion: when the pH reached the upper limit (setpoint plus hysteresis), the actuator was triggered to inject CO_2 into the solution; when the pH reached the lower limit (setpoint minus hysteresis), the actuator was deactivated, stopping the CO_2 injection.

Based on the literature, three initial pH ranges were defined to analyze microalgae growth (Trivedi et al., 2019). Each range was tested in distinct cultures, with duplicates for each condition. The pH values ranged from 6.0 to 9.0, with setpoint of 7.5, as follows:

Cultivation 1: Hysteresis amplitude effects on *Scenedesmus obliquus* BR003 growth.

- Range 1: ΔpH 7.0–8.0 (Lower limit 7.0, setpoint 7.5, upper limit 8.0, hysteresis 0.5) → samples S1 and S4.
- Range 2: ΔpH 6.5–8.5 (Lower limit 6.5, setpoint 7.5 upper limit 8.5, hysteresis 1.0) → samples S2 and S5.
- Range 3: ΔpH 6.0–9.0 (Lower limit 6.0, setpoint 7.5 upper limit 9.0, hysteresis 1.5) → samples S3 and S6.

Based on the results from cultivation 1, which was carried out over a period of 28 days (detailed in the results section), the hysteresis value that yielded the highest microalgae growth (0.5) was selected for the second experimental stage. The subsequent stage, conducted over 36 days, involved shifting the setpoint by ± 0.5 pH units within the range that provided similar microalgae growth (pH 6.5 to 8.5). This allowed us to evaluate new ranges, also in duplicates:

Cultivation 2: Exploratory study with a hysteresis of 0.5.

- Control Range: ΔpH 7.0–8.0 (Lower limit 7.0, setpoint 7.5, upper limit 8.0, hysteresis 0.5) → samples S1 and S4;
- Lower Shifted Range: ΔpH 6.5–7.5 (Lower limit 6.5, setpoint 7.0, upper limit 7.5, hysteresis 0.5) → samples S2 and S5;
- Upper Shifted Range: ΔpH 7.5–8.5 (Lower limit 7.5, setpoint 8.0, upper limit 8.5, hysteresis 0.5) → samples S3 and S6.

For this study, values were treated as the mean of each sample and its duplicate. Therefore, the data sets are denoted as follows:

- S14: data set for S1 and S4;
- S25: data set for S2 and S5;
- S36: data set for S3 and S6.

Growth curves were generated from absorbance measurements at 680 and 750 nm. According to Lu et al. (2017), these were reliable indicators of microalgae growth (Eq. 8):

$$y(t) = \frac{K'}{1 + a'e^{-b't}} \quad (8)$$

Where:

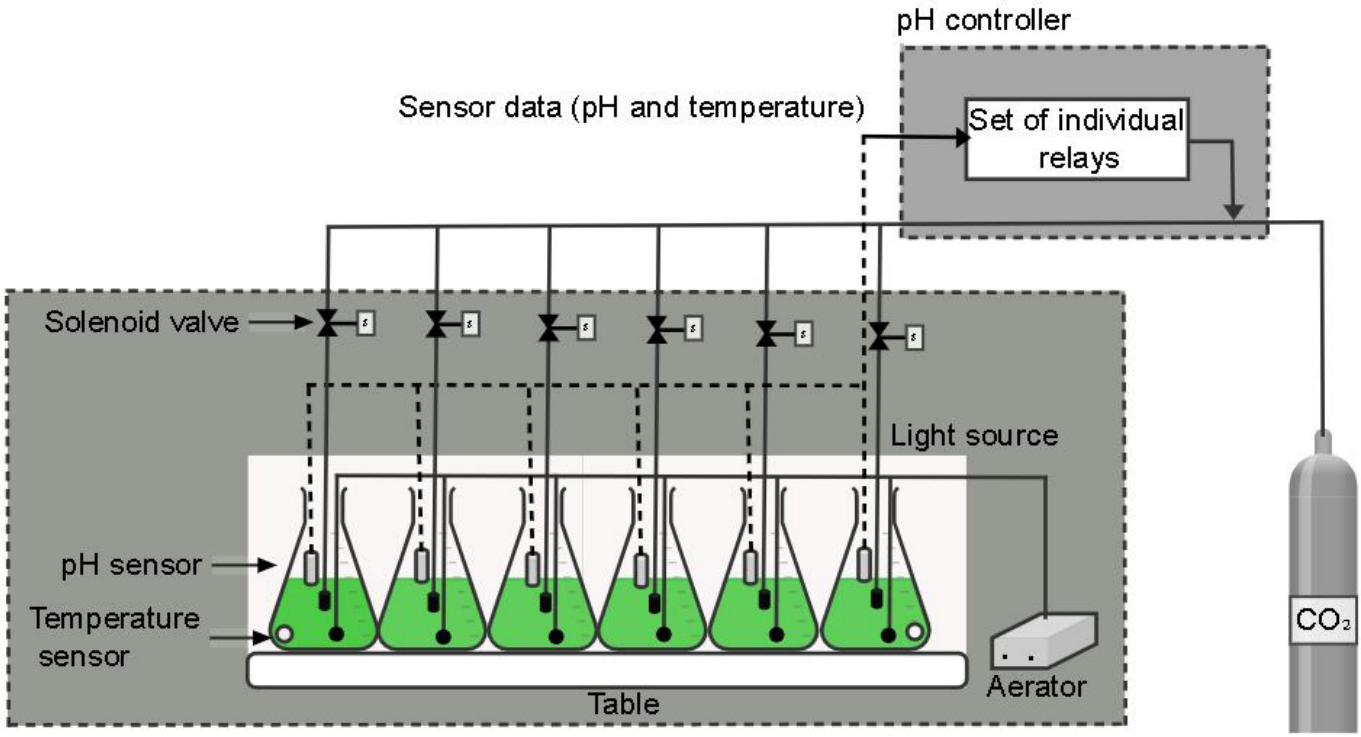

Figure 1. Schematic diagram of the general experimental setup used for microalgae cultivation in both procedures

y(t) – Biomass (or cell density) as a function of cultivation time (t), expressed in Absorbance Units (AU) [or g L^{-1}];

K' - Carrying capacity of the medium (maximum asymptotic value), expressed in the same unit as y(t) (e.g., AU or g L^{-1});

a' - Parameter related to the initial biomass y(0), defined by the expression $a' = \frac{K}{y(0)} - 1$; as it represents a ratio of identical units, it is dimensionless;

b` - Intrinsic specific growth rate, expressed in inverse time, per day, and,

t - Cultivation time (days).

This model was chosen for its ability to accurately describe the classic phases of microbial growth - lag, exponential, and stationary - in a continuous manner. Furthermore, fitting this curve allows for the precise estimation of key parameters, such as the growth rate and maximum biomass, enabling a direct comparison of the effects of pH on the different cultivation conditions.

The dry mass (g L^{-1}) of the culture was determined according to the method described by Rocha et al. (2023). First, 0.22 µm filters were dried in an oven at 60 °C for 24 hours and then weighed on a precision balance in a closed environment to prevent moisture absorption. After this preparation, a 10 mL sample of the culture was filtered. The filter with the retained biomass was then returned to the oven at 60 °C, kept for another 24 hours and weighed again. The dry mass was calculated as the difference between the final weight of the filter with biomass and the initial dry weight of the filter. The value was expressed in g mL^{-1} and converted to g L^{-1}, representing cellular productivity. For each pH range, two samples were analyzed, and the final dry mass value was calculated as a simple arithmetic mean.

The CO_2 control system comprised six solenoid valves, with two valves dedicated to each of the three pH treatments (one for the primary photobioreactor and one for its replicate). Each valve was experimentally verified to consume 0.9 (A) at 12 (V), resulting in a power consumption of 10.8 (W) per unit. To prevent electrical overload and ensure stable voltage, the valves were powered by two independent 12 (V) power supplies, each supporting three valves. All activation and deactivation events were recorded in real-time using a Real-Time Clock (RTC) module and an SD card. A custom Python script was developed to process the log files and calculate the cumulative activation time (t_{on}) for each individual valve over the entire cultivation period. The total energy consumption (E) in Watt-hours (Wh) was calculated as: $E = 10.8\ (W) \times t_{on}$. This value was normalized by the final dry biomass produced, providing the specific energy consumption in Wh mg^{-1}.

A non-linear logistic regression model based on the proposed by Trivedi et al. (2019) was used. The regression analysis and statistical comparisons were performed using Python software version 3.11.5 (Python Software Foundation) within the Spyder Integrated Development Environment (IDE). Additionally, CO_2 pump activation charts, were generated using R software within the RStudio IDE version 2025.05.1 (Posit Software, PBC). Specifically, data importation and temporal processing were conducted using readxl (Wickham & Bryan, 2023) and lubridate (Spinu et al., 2023), while data manipulation and visualization were performed using dplyr (Wickham et al., 2023a) and ggplot2 (Wickham, 2016). Typographical formatting and high-resolution vector graphics export were handled by the extrafont (Chang, 2023) and svglite (Wickham et al., 2023b) packages, respectively.

The biomass production results were compared among the different pH treatments, hysteresis ranges, and cultivation days by analysis of variance and Tukey's test at a $p \leq 0.05$.

Results and Discussion

Before detailing the specific effects of the hysteresis bands, it is essential to evaluate the overall growth kinetics of *Scenedesmus obliquus* under the varying pH conditions. Recent studies emphasize that dynamic pH fluctuations during CO_2 injection directly impact both cellular proliferation and photosynthetic pigment synthesis (Khan et al., 2024; Maghzian et al., 2024). To accurately capture these biological responses, optical density was monitored at two distinct wavelengths: 680 nm, which reflects chlorophyll-a absorption and photosynthetic activity, and 750 nm, which accounts for overall cellular turbidity and biomass accumulation (Isiramen et al., 2022). In this context, the parameters obtained from the logistic regression for *Scenedesmus obliquus* BR003 growth in cultivation 1 are presented in Table 1, which includes data for both 680 nm and 750 nm wavelengths.

Table 1 displays the regression parameters, asymptote (k), a, and growth rate (b) for the three culture conditions (S14, S25, and S36) at both wavelengths. Notably, the S14

Table 1. Estimated parameters of the fitted model for cultivation 1 at 680 and 750 nm

Cultivation	680 nm			750 nm		
	Asymptote (k)	a	b (rate)	Asymptote (k)	a	b (rate)
S14	1.35 (1.26 - 1.44)	9.78 (7.66 - 11.9)	0.17 (0.15 - 0.19)	0.540 (0.51 - 0.57)	10.17 (8.0 - 12.34)	0.18 (0.16 - 0.20)
S25	1.03 (0.94 - 1.12)	9.54 (8.05 - 11.03)	0.14 (0.12 - 0.16)	0.40 (0.38 - 0.42)	10.58 (9.19 - 11.97)	0.16 (0.14 - 0.18)
S36	1.03 (0.95 - 1.11)	8.92 (7.59 - 10.25)	0.15 (0.13 - 0.17)	0.42 (0.39 - 0.45)	9.77 (8.42 - 11.12)	0.16 (0.14 - 0.18)

S14 - Range 1 (pH 7.0–8.0, hysteresis 0.5); S25 - Range 2 (pH 6.5–8.5, hysteresis 1.0); S36 - Range 3 (pH 6.0–9.0, hysteresis 1.5); k - Carrying capacity (absorbance); b - Specific growth rate (d^{-1}); a - Integration constant. Values are presented with their respective 95% confidence intervals (CI), calculated from logistic regression

culture exhibited the highest values for both the asymptote and growth rate at 680 nm, suggesting superior growth performance under this condition. However, absorbance at 680 nm is primarily associated with chlorophyll content and photosynthetic activity, not total biomass. In contrast, measurements at 750 nm, which is more directly related to biomass concentration, provide a more appropriate basis for comparing growth among treatments (Griffiths et al., 2011). The comparison among culture conditions was based on the estimated parameters of the fitted models, and differences were interpreted descriptively. However, to define the overall 'optimal' conditions across the cultivations, this study evaluates both biological performance (biomass) and control system efficiency (energy consumption)

As highlighted by Lu et al. (2017), this spectral range is particularly suitable for evaluating pigment concentrations and photosynthetic efficiency. Therefore, while S14 showed higher values at 680 nm, these results should be interpreted alongside more direct biomass indicators, such as absorbance at 750 nm.

The data at 750 nm, also included in Table 1, provide a more accurate estimation of total biomass due to minimal interference from photosynthetic pigments. At this wavelength, S14 showed higher mean absorbance, asymptote (k), and growth rate (b) compared to the other conditions, indicating a trend toward greater biomass accumulation. In contrast, S25 and S36 showed consistently lower values across all parameters, suggesting lower biomass accumulation.

Considering the results obtained, particularly at 750 nm, S14 can be considered a promising condition for biomass production. These patterns can be explained by the relationship between microalgal carbon uptake and carbon availability in the medium. Microalgae assimilate inorganic carbon mainly as CO_2 and HCO_3^-, which are used in photosynthesis and biomass formation (Wang et al., 2023; Udaypal et al., 2024). Thus, growth is directly influenced by the availability and forms of inorganic carbon in the medium. From a process perspective, these carbon forms depend on pH and mass transfer, which control CO_2 dissolution and its equilibrium with bicarbonate (Kong et al., 2021; Maghzian et al., 2024). These trends are visually supported by the fitted growth curves at 750 nm (Figure 2A) and 680 nm (Figure 2B).

Additionally, a pH range of 7.0 to 8.0, corresponding to a hysteresis of 0.5, yielded optimal outcomes in terms of both photosynthetic activity (680 nm) and biomass accumulation (750 nm). This suggests that maintaining pH within a narrow range can be effective for on-off control systems, minimizing unnecessary switching.

The growth curves and model fitting shown in Figure 2 are consistent with the known influence of pH on microalgal growth. pH affects carbon availability, enzyme activity, and nutrient uptake, with most species exhibiting optimal growth under neutral to slightly alkaline conditions (Maghzian et al., 2024). Therefore, the evaluated pH ranges are supported by established microalgae cultivation practices.

Figure 3 shows the activation of the CO_2 injection valve in response to pH fluctuations. It demonstrates the controller's operation for the pH range of 6.5 to 7.5 in culture S2 in August.

The graph illustrates two activation events where the pH reached the upper limit (7.5), triggering CO_2 injection until the pH dropped to 7.0. A further drop, approaching pH 6.0, was observed after each deactivation; this overshoot is attributed to process inertia from CO_2 dissolution, compounded by the dynamics of the carbonate equilibrium. Specifically, the continuous hydration of the dissolved CO_2 into carbonic acid temporarily overwhelms the medium's buffering capacity, causing the pH to keep dropping even after the gas injection is halted. Although the experiment was conducted in bench-scale flasks, the control dynamics resemble those reported by Rodríguez-Torres et al. (2021) in larger-scale systems such

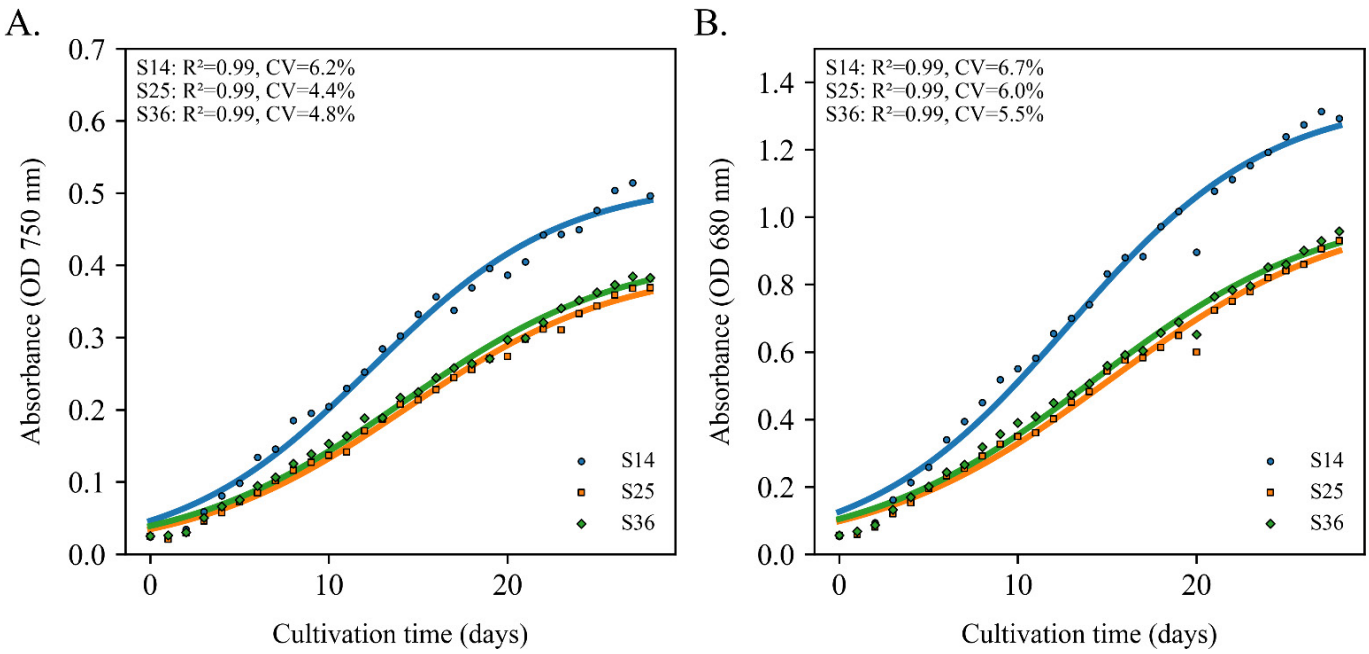

S14 - Range 1 (pH 7.0–8.0, hysteresis 0.5); S25 - Range 2 (pH 6.5–8.5, hysteresis 1.0); S36 - Range 3 (pH 6.0–9.0, hysteresis 1.5); R^2 - Coefficient of determination; CV - Coefficient of variation

Figure 2. Logistic regression for biomass growth at 750 and 680 nm in cultivation 1

as raceways and thin-layer photobioreactors. This overshoot behavior highlights the practical implications of hysteresis in on-off control systems and the need to account for transients beyond the set limits, especially when applying traditional control strategies like PI controllers.

Despite the transient drops, no significant differences were found between the overshoot levels of different hysteresis ranges or culture ages (ANOVA, $p = 0.98$). However, a statistically significant difference was observed in the minimum pH values across cultivation days ($p \leq 0.001$). Post-hoc Tukey's test revealed that, in culture S2, the minimum pH on day 36 was significantly lower than on day 1 ($\Delta = -0.16$; $p \leq 0.001$) and day 18 ($\Delta = -0.21$; $p \leq 0.001$), suggesting that the system's response to CO_2 injection changes over time, possibly due to changes in carbon uptake and physicochemical condition of the culture.

The logistic regression parameters for Cultivation 2, based on absorbance at 680 nm and 750 nm, are presented in Table 2.

Among the tested conditions, S25 (pH 6.5–7.5) showed the best overall performance, with the highest growth rate ($b = 0.10$) and asymptote ($k = 1.62$). The S14 culture (pH 7.0–8.0) had similar results, while S36 (pH 7.5–8.5) exhibited a high asymptote ($k = 3.61$) but lower growth rate ($b = 0.07$) due to an extended lag phase. This initial stagnation lasted for about one-third of the total cultivation time, but the culture eventually recovered, suggesting that adaptation time, not potential, limited performance. This phenomenon is consistent with the metabolic physiological adjustments required during the lag phase, as cells reorganize their enzymatic machinery to cope with new environmental conditions before entering the exponential growth stage (Andersen, 2005).

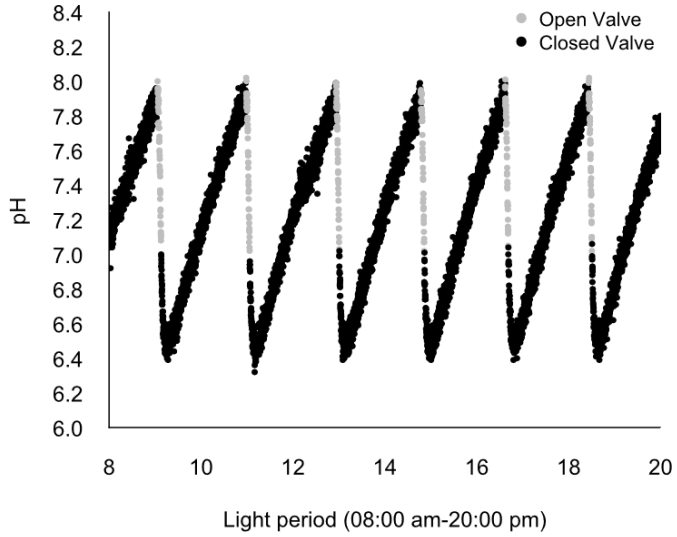

Figure 3. pH profile in the S2 cultivation system during the light period (08:00 a.m. –08:00 p.m.), with solenoid valve activation controlled within the range of 6.5–7.5 using a 0.5 hysteresis band

These findings contrast with those from cultivation 1 as with the hysteresis kept constant, the pH range itself directly influenced microalgal growth dynamics. The slightly higher performance of S25 over S14 indicates that the optimal pH window for maximizing biomass production may lie between 6.5 and 8.0 (Table 2).

These trends are also reflected in Figure 4, which shows the growth curves based on absorbance at both wavelengths. The overall growth patterns were consistent, with S25 outperforming the others across both indicators.

Among the treatments, S25 (pH 6.5–7.5) demonstrated slightly superior performance compared to S14 (pH 7.0–8.0), while S36 (pH 7.5–8.5) showed delayed growth but recovered after the tenth day (Figures 4A and B). Its growth rate, however, remained approximately 30% lower than that of S25. These results indicate that, unlike in cultivation 1, the position of the hysteresis range (pH window) in cultivation 2 had less impact than the width of the range.

Overall, the pH 6.5–7.5 range proved to be the most effective for both photosynthetic efficiency and biomass accumulation, making it the most promising for application in on-off control systems with hysteresis.

Table 3 presents the average dry biomass obtained for each treatment in Cultivation 2, including standard deviations and Tukey's post-hoc test results. The data confirm the trends observed in the absorbance-based growth curves.

Significant differences between samples were verified ($p \leq 0.01$). According to Tukey's test (Table 3), S36 had significantly lower biomass compared to both S14 and S25, while there was no significant difference between S14 and S25.

Additionally, the lower performance of S36 appears to be associated with a pronounced lag phase in the initial days of cultivation. While the specific cause was not identified in this study, this early inhibition may be related to the upper limit of the hysteresis range (pH 8.5), which can alter the availability of inorganic carbon species in the medium.

Table 2. Estimated parameters of the fitted model for cultivation 2 at 680 and 750 nm

Cultivation	680 nm			750 nm		
	Asymptote (k)	a	b (rate)	Asymptote (k)	a	b (rate)
S14	1.54 (1.4 - 1.74)	9.63 (8.73 - 10.53)	0.09 (0.08 - 0.10)	0.54 (0.49 - 0.59)	8.68 (7.87 - 9.49)	0.09 (0.08 - 0.10)
S25	1.62 (1.48 - 1.76)	10.26 (9.25 - 11.27)	0.10 (0.09 - 0.11)	0.60 (0.55 - 0.65)	10.09 (9.10 - 11.08)	0.10 (0.09 - 0.11)
S36	3.61 (0.37 - 6.85)	43.59 (9.8 - 77.38)	0.07 (0.06 - 0.08)	1.17 (0.53 - 1.81)	31.35 (16.68 - 46.02)	0.07 (0.06 - 0.08)

S14 - Control Range (setpoint 7.5, pH 7.0–8.0); S25 - Lower Shifted Range (setpoint 7.0, pH 6.5–7.5); S3S6 - Upper Shifted Range (setpoint 8.0, pH 7.5–8.5); k - Carrying capacity (absorbance); b - Specific growth rate (d^{-1}); a -Integration constant. Values are presented with their respective 95% confidence intervals (CI), calculated from logistic regression

At higher pH values, dissolved CO_2 becomes less available, with a shift toward bicarbonate (HCO_3^-), which is not equally utilized by all microalgae, potentially limiting photosynthetic efficiency and initial growth (Markou et al., 2014). Nevertheless, the observed recovery and subsequent growth indicate that this condition could still be viable if supported by adaptation or acclimation strategies. This behavior may be related to the ability of microalgae to adapt to suboptimal cultivation conditions, particularly those affecting carbon availability and pH, where an initial inhibition phase may be followed by physiological adjustment and subsequent recovery (Paliwal et al., 2017; Maghzian et al., 2024)

Some general statistical characteristics of cultivation 1 and cultivation 2 are presented in Table 4. The mean pH of the cultures remained closer to the lower limit, but still within the stipulated range. This is due to culture's inertia in responding to CO_2 injection. The longest CO_2 valve activation time was observed in the S14 culture, suggesting more intense metabolic activity, possibly in response to a more acidified environment. The shorter activation times for S25 and S36 were due to their wider hysteresis ranges, indicating that these cultures required more time to adapt. The average daily temperature in the laboratory was 22.79 °C, which did not directly influence the differences observed among the treatments.

Cultivation 1 and 2 lasted 28 and 36 days, respectively. These durations were longer than the 15 to 18 days typically reported in literature for complete microalgal growth assessments. For instance, the foundational protocols described by Andersen (2005) are primarily optimized for strictly controlled laboratory batch cultures, maintained under ideal and constant physiological conditions to maximize rapid exponential growth.

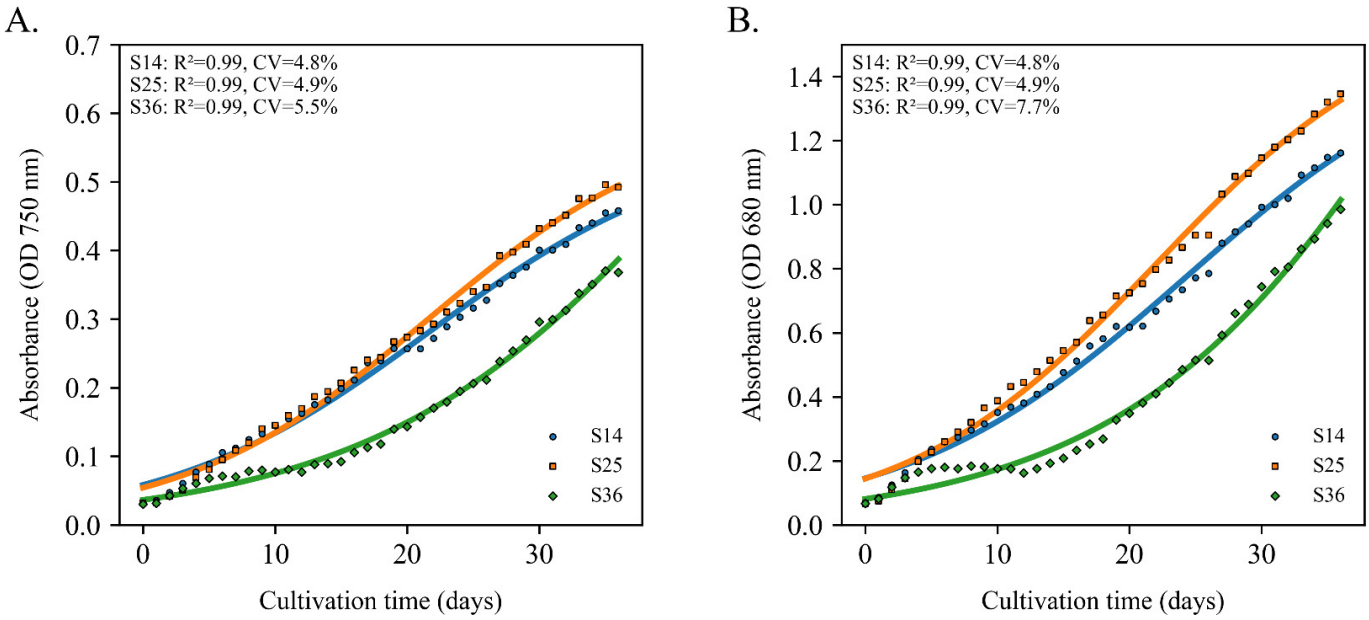

S14 - Control Range (setpoint 7.5, pH 7.0–8.0); S25 - Lower Shifted Range (setpoint 7.0, pH 6.5–7.5); S36 - Upper Shifted Range (setpoint 8.0, pH 7.5–8.5); R^2 - Coefficient of determination; CV (%) - Coefficient of variation

Figure 4. Logistic regression curves for microalgal growth based on absorbance at 750 nm and 680 nm for the three pH treatments - Cultivation 2

Table 3. Average dry weight of microalgal biomass for cultivations S14 to S36 and Tukey's test results for sample growth

Cultivation	pH Range	Mean productivity (g L^{-1}) ± SD	Tukey (5%)
S14	7 – 8	0.97 ± 0.05	a
S25	6.5 - 7.5	1.02 ± 0.08	a
S36	7.5 - 8.5	0.85 ± 0.03	b

S14: Control Range (setpoint 7.5, pH 7.0–8.0); S25: Lower Shifted Range (setpoint 7.0, pH 6.5–7.5); S3S6: Upper Shifted Range (setpoint 8.0, pH 7.5–8.5)

Table 4. General characteristics of cultivation 1 and cultivation 2

Characteristic	Samples					
	Cultivation 1			Cultivation 2		
	S14	S25	S36	S14	S25	S36
Average pH	7.59	7.88	8.13	7.22	6.9	7.81
CO_2 valve injection time (hours)	15.93	12.04	13.01	21.04	41.04	16.82
Power consumption of the control system (W h^{-1})	152.76	115.46	124.76	201.94	393.94	161.42
Average ambient temperature (ºC)	22.79	22.79	22.79	21.1	21.1	21.1

S14 - Control Range (setpoint 7.5, pH 7.0–8.0); S25 - Lower Shifted Range (setpoint 7.0, pH 6.5–7.5); S3S6 - Upper Shifted Range (setpoint 8.0, pH 7.5–8.5)

Furthermore, recent studies such as Caparroz et al. (2024), which also report shorter cultivation cycles, utilized open raceway reactors equipped with advanced data-driven predictive models and adaptive pH control systems that dynamically optimize the environment. In contrast, the extended cultivation periods required in the present study reflect our specific, cost-effective operational conditions. The use of commercial agricultural fertilizers, tap water, and the intentional introduction of pH hysteresis ranges demanded longer cellular acclimatization periods (lag phase), naturally extending the time required to reach the maximum carrying capacity.

However, a study by Song et al. (2019) on *Chlorella* sp. also ran for 36 days but used ammonia (NH_4HCO_3) as the source for both CO_2 and nitrogen. This contrasts with the present study, where CO_2 was injected via hysteresis control and ammonia was added as a solution at the beginning of the cultivation.

The extended experimental time in the present study was justified by several factors: the need for system stabilization to precisely select pH ranges; the CO_2 flow rate had to be low to ensure the influence of hysteresis variation; the complexity of the hysteresis phenomenon, which involves physiological and metabolic responses with memory and temporal delays that cannot be captured in shorter periods (Prasad et al., 2021; Isiramen et al., 2022).

Initial oscillations and growth lag, particularly in the pH 7.5–8.5 range, required prolonged observation to ensure reliable results. This was also noted in studies that highlight the influence of environmental conditions and control strategies on algal performance (Rodríguez-Miranda et al., 2020; Khan et al., 2024). Finally, the inherent variability in biotechnological systems and methodological differences between studies, such as microalgae strain, culture conditions, equipment, and monitored parameters, also play a role (Borowiak et al., 2020; Estevam et al., 2023).

Consequently, experimental timelines must be adapted to the specific system. For instance, while we cultivated *Scenedesmus obliquus* under pH hysteresis constraints, similar adaptations in cultivation time were reported by Trivedi et al. (2019), when studying the same species under varying irradiance levels. Furthermore, Tripathi et al. (2015) and Song et al. (2019) highlighted the need for prolonged monitoring when cultivating *Scenedesmus* sp. for CO_2 sequestration and nutrient limitations. These comparisons demonstrate that environmental stressors—whether related to carbon availability, light or pH control—directly induce extended lag phases that require tailored observation periods.

According to Table 4, the mean pH of the cultures remained closer to the lower limit but within the specified range, which reflects the system's inertia in responding to CO_2 injection. The S25 culture required the longest CO_2 injection time (41.04 hours), indicating more intense metabolic activity, possibly in response to a more acidified environment. In contrast, the S14 culture required approximately half the activation time (21.04 hours) with nearly identical growth, suggesting a potential balance between stimulus and response. Regarding environmental conditions, the average laboratory temperature was 22.79 °C during Cultivation 1 and 21.1 °C during Cultivation 2; these minor thermal variations did not directly influence the observed differences among treatments.

Considering that cultivation 2 was conducted to identify the most suitable setpoint options for microalgae cultivation, energy consumption is a crucial factor for selecting controller parameters. The energy consumption per milligram for each cultivation 2 sample was as follows: S14 - 0.21 W mg^{-1}; S25 – 0.39 W mg^{-1}; and S36 – 0.19 W mg^{-1}. These results suggest that, from an energy perspective, the S14 parameterization is more advantageous. It provides similar productivity to S25 while consuming a similar amount of energy as S36. This reinforces the idea that S14 operates at or near an equilibrium point for CO_2 injection and productivity. Compared to S25, S14's control system consumes 46.7% less energy, making it a relevant parameterization option. Energy consumption is a critical consideration as it relates not only to operational costs but also to hardware costs, component selection, battery life, and the sizing of off-grid power systems.

The results of this study indicate that the pH range of 6.5 to 7.5 yielded the highest average biomass, with a dry mass of 1.02 g L^{-1}. This value is statistically equivalent to that obtained with the 7.0 to 8.0 range, which produced 0.97 g L^{-1}. This trend was also reflected in the absorbance at 680 nm, which was higher in the 6.5–7.5 range, suggesting a greater concentration of pigments and higher photosynthetic efficiency. These findings corroborate previous work that identifies pH ranges near neutral or slightly acidic as being more favorable for microalgae growth and metabolic activity (Lu et al., 2017; Estevam et al., 2023).

The prolonged activation time and higher energy consumption observed in the intermediate pH ranges indicate greater metabolic activity under these conditions, underscoring the importance of pH control for maximizing algal productivity (Khan et al., 2024). These findings were consistent with observations from Rodríguez-Miranda et al. (2020) and Isiramen et al. (2022), who highlight the influence of pH control and stability on the efficiency of cultivation systems for microalgae species such as *Scenedesmus* sp.

In the pH 7.5–8.5 range, the occurrence of oscillations and an initial growth lag, stabilizing only after the tenth day, highlights the system's sensitivity to environmental variations. This is likely due to adaptive processes and physiological stress. This observation aligns with studies by Prasad et al. (2021) and Khan et al. (2024), which emphasize the importance of maintaining pH stability to avoid delayed responses and productivity loss. The presence of hysteresis in algal growth reinforces the existence of physiological memory and adaptation, which are fundamental for developing adaptive pH control strategies, as noted by Rodríguez-Torres et al. (2021) and Caparroz et al. (2024). The system's ability to respond differently to increasing versus decreasing pH trajectories demonstrates the biological complexity that must be considered in cultivation management.

The similarity between the dry mass and absorbance values for the present study and those reported in the

literature supports the reliability of the applied methods. Lu et al. (2017) reported correlation between optical density and dry biomass, indicating that absorbance at 680 nm is mainly related to chlorophyll content, while higher wavelengths provide a better estimation of biomass. A similar consistency between optical measurements and microalgal growth was also observed by Borowiak et al. (2020) under controlled conditions. In this context, the agreement between dry mass and absorbance observed in the present study reinforces the adequacy of the monitoring approach and supports the validity of the experimental results. The controllers effectively implemented hysteresis in the cultures, aligning with best practices for this type of experiment.

The growth observed in S14 suggests an optimal setpoint zone for cultivation (pH 7.0 to 7.5), while S25 maintained higher photosynthetic and metabolic activity, as indicated by its absorbance and prolonged activation time. The oscillation and growth lag in the 7.5–8.5 range point to adaptive responses and potential physiological limitations when the system is initially exposed to higher pH levels.

Khan et al. (2024) studied a low-cost pH control system based on an Arduino microcontroller and a relay-controlled solenoid valve. The device was programmed to inject CO_2 when the pH exceeded 8.3 and cease injection when the value dropped below 7.0, characterizing on-off control with hysteresis. The system was tested in 200 L raceway ponds for the cultivation of *Geitlerinema* sp. and *Spirulina* sp., resulting in increased biomass density compared to uncontrolled cultures. However, it is noteworthy that their study evaluated on-off control with fixed hysteresis without exploring different ranges. In contrast, the present work investigates the impact of varying these ranges on the cultivation process.

In Rodríguez-Miranda et al. (2020), an on-off controller was compared to a dual-period PI controller (diurnal and nocturnal) in a raceway pond. It was concluded that PI control yielded superior results. However, hysteresis was not utilized in the on-off control comparison. Rodríguez-Torres et al. (2021) compared on-off and PI controllers for pH control in thin-layer and raceway tanks. The PI controller provided better pH stability in both cases, including during the nocturnal period. However, the current research proposes an ideal operational range containing multiple potential setpoints that can be utilized without productivity losses; thus, system stability at a single setpoint is not the primary objective. This approach allows for greater control system flexibility, enabling setpoint variations according to external factors (e.g., temperature, and radiation) and promoting optimizations in both productivity and operational factors, such as energy consumption.

Among studies effectively applying on-off control with hysteresis to microalgae, two recent examples stand out. In Caparroz et al. (2024), the method was used in raceway reactors with hysteresis limits set at 8.3 and 7.7, primarily as an experimental reference for process characterization and subsequent PI autotuning development. In Isiramen et al. (2022), on-off control with hysteresis was applied to a raceway system alongside a novel PI+dead-zone control scheme for comparative purposes. In that case, the on-off strategy exhibited significant oscillations around the setpoint (pH 6.5) and higher CO_2 consumption, although biomass productivity remained similar. While interest in hysteresis-based control is growing in recent research, systematic studies on the influence of different ranges and intervals remain scarce, a gap addressed by the present research.

Borowiak et al. (2020) employed on-off control with a fixed 0.2 hysteresis to maintain pH at 7.0 during the automated cultivation of *Haematococcus pluvialis* in airlift photobioreactors. They utilized CO_2 injection for pH adjustment and developed a modular automated station for inoculum preparation, achieving high productivity and process stability. In contrast, the principle of on-off control with hysteresis is applied in this work to *Scenedesmus obliquus* cultivation, also using CO_2 injection, but with the objective of investigating different ranges and their impact on pH control performance to broaden the understanding of this optimization strategy.

Studies such as Tripathi et al. (2015), using *Scenedesmus* sp., demonstrated that pH 8.0 promotes higher biomass production compared to other ranges (tested from pH 7.0 to 10.0). Chiranjeevi & Mohan (2016) obtained similar results with an optimal pH of 8.5. These findings suggest that small variations around these values can significantly impact cell growth rates. Therefore, the parameterization of hysteresis around these optimal points may represent an efficient control strategy, provided it is based on technical-scientific criteria.

Rodríguez-Torres et al. (2021), using on-off control, highlighted the non-linear nature of the cultivation process and variations in system behavior between diurnal and nocturnal periods. These results indicate that adopting well-defined hysteresis bands may contribute to adapting control to environmental and biological fluctuations. Consequently, while on-off control with hysteresis has been used in large-scale applications, primarily as a baseline for comparison with advanced strategies, the present study focuses on the behavior of the controller itself. The impact of different hysteresis values on microalgae cultivation was experimentally investigated.

To define the overall optimal condition for the automated cultivation of *Scenedesmus obliquus* BR003, it is necessary to evaluate the balance between biological performance and control system efficiency. According to the biomass productivity data (Table 3), the S25 and S14 culture are suitable for microalgal growth.

As presented in Table 4, maintaining the pH between 6.5 and 7.5 (S25) required 41.04 hours of CO_2 valve activation, resulting in an energy consumption of 393.94 Wh by the control system. In contrast, the 7.0–8.0 range (S14) required only 21.04 hours of injection, consuming 201.94 Wh. This demonstrates that shifting the pH setpoint from 7.0 to 7.5 (while keeping the 0.5 hysteresis) reduced energy consumption and actuator wear by approximately 48.7%.

Therefore, a clear trade-off is established: while pushing the pH to a slightly more acidic range (6.5–7.5) maximizes carbon availability and pushes biological yield to its absolute limit, it does so at an unsustainable energy cost. Considering the lack of statistical difference in biomass production, the

7.0–8.0 range (S14) is defined as the overall optimal condition, balancing high productivity with significant operational and energy savings.

While these findings optimize the on-off controller behavior, future studies should focus on validating this trade-off in larger-scale photobioreactors, evaluating system dynamics during nocturnal periods, and exploring the integration with industrial CO_2 emission sources to further confirm large-scale feasibility.

Conclusions

1. Hysteresis directly influences the frequency of CO_2 valve activation, the energy consumption of the pH control system, and the biomass productivity of *Scenedesmus obliquus* BR003.

2. Biomass productivity did not differ statistically between the pH ranges of 6.5–7.5 and 7.0–8.0. These results indicate that pH ranges close to neutrality are suitable for maximizing productivity in *Scenedesmus obliquus* BR003.

3. Considering the balance between biomass production and operational efficiency, the pH range of 7.0–8.0 is recommended for the automated cultivation of *Scenedesmus obliquus* BR003, as it maintained productivity comparable to the 6.5–7.5 range while reducing energy consumption and actuator wear.

Contribution of authors: Souza, E. M. de: investigation, data curation, writing - original draft. Oliveira, J. V. P.: methodology, validation, resources, writing - review & editing, supervision, funding acquisition, project administration. Carmo, P. H. do: investigation, data curation, writing - original draft, writing - review & editing. Rocha, D. N.: conceptualization, methodology, resources. Martins, M. A.: conceptualization, methodology, software, formal analysis, supervision.

Data Availability Statement: The authors declare that there are no data underlying the text.

Conflict of Interest: None to declare.

Financing statement: This study was financed in part by the Coordenação de Nível Superior - Brazil (CAPES) - Finance Code 001- and by Fundação de Amparo à Pesquisa do Estado de Minas Gerais (FAPEMIG) (Grant APQ-02187-24).

Acknowledgments: The authors thank the Federal University of Viçosa (UFV) for providing the physical space and institutional support. We also thank FAPEMIG (Grant APQ-02187-24) for the research scholarship and materials, and CAPES for the financial support to the Graduate Program in Agricultural Engineering at UFV.

Literature Cited

Andersen, R. A. (ed.). Algal culturing techniques. 1.ed. Burlington, MA: Elsevier Academic Press. 2005. 578p.

Borowiak, D. et al. Propagation of inoculum for *Haematococcus pluvialis* microalgae scale-up photobioreactor cultivation system. Applied Sciences, v.10, 6283, 2020. https://doi.org/10.3390/app10186283

Caparroz, M. et al. A novel data-driven model for prediction and adaptive control of pH in raceway reactor for microalgae cultivation. New Biotechnology, v.82, p.1–13, 2024. https://doi.org/10.1016/j.nbt.2024.04.001

Chang, W. Extra font: Tools for using fonts. R package version 0.19. 2023. Available on: https://CRAN.R-project.org/package=extrafont. Accessed on: Apr. 2025.

Chiranjeevi, P.; Mohan, S. V. Critical parametric influence on microalgae cultivation towards maximizing biomass growth with simultaneous lipid productivity. Renewable Energy, v.98, p.64-71, 2016. https://doi.org/10.1016/j.renene.2016.03.063

DIN - Deutsches Institut für Normung. pH measurement - reference buffer solutions for the calibration of pH measuring equipment. 2015. Available on: https://www.din.de/. Accessed on: Apr. 2026.

Estevam, B. R. et al. Effects of cultivation systems and nutrient limitation on the growth and metabolite biosynthesis of *Botryococcus terribilis*. biomass conversion and biorefinery, v.14, p.17251-17262 2023. https://doi.org/10.1007/s13399-023-03805-w

Galster, H. pH measurement: fundamentals, methods, applications, instrumentation. 1.ed. Weinheim: VCH Publishers, 1991. 356p.

Griffiths, M. J. et al. Interference by pigment in the estimation of microalgal biomass concentration by optical density. Journal of Microbiological Methods, v.85, p.119-123, 2011. https://doi.org/10.1016/j.mimet.2011.02.005

Huang, Q. et al. Design of photobioreactors for mass cultivation of photosynthetic organisms. Engineering, v.3, p.318-329, 2017. http://dx.doi.org/10.1016/J.ENG.2017.03.020

Ildefonso, L. L. H. et al. Potential of microalgae cultivation for carbon sequestration and stock associated with biofertilizer production. Biomass and Bioenergy, v.209, 108975, 2026. https://doi.org/10.1016/j.biombioe.2026.108975

Isiramen, O. E. et al. Improving pH control and carbon dioxide utilisation efficiency in microalgae cultivation systems with the use of a proportional-integral + dead-zone control strategy. Bioresource Technology Reports, v.17, 12145, 2022. https://doi.org/10.1016/j.biteb.2021.100917

ISO - International Organization for Standardization. Water quality — determination of pH. 2008. Available on: https://www.iso.org/standard/43173.html. Accessed on: Apr. 2026.

Khan, S. et al. Application note—A novel, low-cost pH-controlled solenoid-based CO_2 dosing device for microalgal and cyanobacterial cultivation systems. Smart Agricultural Technology, v.7, 14244, 2024. https://doi.org/10.1016/j.atech.2023.100373

Kong, W. et al. Review on carbon dioxide fixation coupled with nutrients removal from wastewater by microalgae. Journal of Cleaner Production, v.292, 125975, 2021. https://doi.org/10.1016/j.jclepro.2021.125975

Lan, X. et al. Thoning: Trends in globally-averaged CO_2 determined from NOAA global monitoring laboratory measurements. Version Thursday, 05-Mar-2026 10:03:59 MST https://doi.org/10.15138/9N0H-ZH07

Lu, L. et al. A comparative study on three quantitating methods of microalgal biomass. Indian Journal of GeoMarine Sciences, v.46, p.2265–2272, 2017.

Maghzian, A. et al. A comprehensive review on effective parameters on microalgae productivity and carbon capture rate. Journal of Environmental Management, v.355, 120539, 2024. https://doi.org/10.1016/j.jenvman.2024.120539

Markou, G. et al. Microalgal and cyanobacterial cultivation: The supply of nutrients. Water Research, v.65, p.186-202, 2014. https://doi.org/10.1016/j.watres.2014.07.025

Molina, E. et al. Tubular photobioreactor design for algal cultures. Journal of Biotechnology, v.92, p.113-131, 2001. https://doi.org/10.1016/S0168-1656(01)00353-4

Mubarak, M. et al. Bubble column photobioreactor for *Chlorella pyrenoidosa* cultivation and validating gas hold-up and volumetric mass transfer coefficient. Energy Sources, Part A: Recovery, Utilization, and Environmental Effects, v.10, p.9779-9793 2019. https://doi.org/10.1080/15567036.2019.1680769

Ogata, K. Modelagem matemática de sistemas de controle. In: Ogata, K. Engenharia de controle moderno. 5.ed. Boston: Prentice Hall, 2011. Cap.2, p.18–20.

Paliwal, C. et al. Abiotic stresses as tools for metabolites in microalgae. Bioresource Technology, v.244, p.1216-1226, 2017. https://doi.org/10.1016/j.biortech.2017.05.058

Prasad, R. et al. Role of microalgae in global CO_2 sequestration: Physiological mechanism, recent development, challenges, and future prospective. Sustainability, v.13, 13061, 2021. https://doi.org/10.3390/su132313061

Purnamasari, D. N. et al. Digital moving average filter application for echo signals and temperature. E3S Web of Conferences, v.328, 02007, 2021. https://doi.org/10.1051/e3sconf/202132802007

Qin, Y. et al. Combination of non-sterilized wastewater purification and high-level CO_2 bio-capture with substantial biomass yield of an indigenous *Chlorella* strain. Science of the Total Environment, v.873, 162442, 2023. https://doi.org/10.1016/j.scitotenv.2023.162442

Rocha, D. N. et al. Combination of trace elements and salt stress in different cultivation modes improves the lipid productivity of *Scenedesmus* spp. Bioresource Technology, v.289, art. 121644, 2019. https://doi.org/10.1016/j.biortech.2019.121644

Rocha, D. N. et al. Impacts of organic solvent toxicity on resource recovery from *Scenedesmus obliquus* biomass after lipid extraction. Biomass and Bioenergy, v.177, 106948, 2023. https://doi.org/10.1016/j.biombioe.2023.106948

Rodríguez-Miranda, E. et al. Diurnal and nocturnal pH control in microalgae raceway reactors by combining classical and event-based control approaches. Water Science and Technology, v.82, p.1155–1165, 2020. https://doi.org/10.2166/wst.2020.260

Rodríguez-Torres, M. J. et al. Modelling and pH control in raceway and thin-layer photobioreactors for wastewater treatment. Energies, v.14, 1099, 2021. https://doi.org/10.3390/en14041099

Sierra, C. et al. The fate and transit time of carbon in a tropical forest. Journal of Ecology, v.109, p.2845–2855, 2021. https://doi.org/10.1111/1365-2745.13723

Simonová, A. et al. Uses of on–off controller for regulation of higher-order system in comparator mode. Electrical Engineering, v.99, p.1367–1375, 2017. https://doi.org/10.1007/s00202-017-0610-7

Skoog, D. A. et al. Fundamentals of analytical chemistry. 9.ed. Belmont: Brooks/Cole. 2013. 1072p.

Song, C. et al. Integration of CO_2 absorption with biological transformation via using rich ammonia solution as a nutrient source for microalgae cultivation. Energy, v.179, p.618–627, 2019. https://doi.org/10.1016/j.energy.2019.05.039

Spinu, V. et al. lubridate: Make dealing with dates a little easier. R package version 1.9.3. 2023. Available on: https://CRAN.R-project.org/package=lubridate. Accessed on: Apr. 2024.

Tarafdar, A. et al. Environmental pollution mitigation through utilization of carbon dioxide by microalgae. Environmental Pollution, v.328, 121623, 2023. https://doi.org/10.1016/j.envpol.2023.121623

Tripathi, R. et al. Characterization of microalga *Scenedesmus* sp. ISTGA1 for potential CO_2 sequestration and biodiesel production. Renewable Energy, v.74, p.774–781, 2015. https://doi.org/10.1016/j.renene.2014.09.005

Trivedi, J. et al. Development of a non-linear growth model for predicting temporal evolution of *Scenedesmus obliquus* with varying irradiance. Bioprocess and Biosystems Engineering, v.42, p.2047–2054, 2019. https://doi.org/10.1007/s00449-019-02194-7

Udaypal, G. R. K. et al. Advances in microalgae-based carbon sequestration: Current status and future perspectives. Environmental Research, v.249, 118397, 2024. https://doi.org/10.1016/j.envres.2024.118397

Wang, R. et al. Research progress and application of carbon sequestration in industrial flue gas by microalgae: A review. Journal of Environmental Sciences, v.152, p.14–28, 2025. https://doi.org/10.1016/j.jes.2024.04.018

Wang, Z. et al. Comprehensive understanding of regulatory mechanisms, physiological models and key enzymes in microalgal cells based on various concentrations of CO_2. Chemical Engineering Journal, v.454, 140233, 2023. https://doi.org/10.1016/j.cej.2022.140233

Wickham, H.; Bryan, J. readxl: Read excel files. R package version 1.4.3. 2023. Available on: https://CRAN.R-project.org/package=readxl. Accessed on: Apr. 2025.

Wickham, H. ggplot2: Elegant graphics for data analysis. New York: Springer-Verlag, 2016. Available on: https://ggplot2.tidyverse.org. Accessed on: Apr. 2025.

Wickham, H. et al. dplyr: A grammar of data manipulation. R package version 1.1.4. 2023a. Available on: https://CRAN.R-project.org/package=dplyr. Accessed on: Apr. 2025.

Wickham, H. et al. svglite: An 'SVG' graphics device. R package version 2.1.3. 2023b. Available on: https://CRAN.R-project.org/package=svglite. Accessed on: Apr. 2025.